Contest based on a directed polymer in a random medium

Clément Sire*
Laboratoire de Physique Théorique—IRSAMC, UPS and CNRS, Université de Toulouse, 31062 Toulouse, France
(Received 23 July 2008; revised manuscript received 5 October 2008; published 5 December 2008)

We introduce a simple one-parameter game derived from a model describing the properties of a directed polymer in a random medium. At its turn, each of the two players picks a move among two alternatives in order to maximize its final score, and minimize the opponent's return. For a game of length n, we find that the probability distribution of the final score S_n develops a traveling wave form, $\text{Prob}(S_n=m)=f(m-vn)$, with the wave profile $f(z)$ decaying unusually as a double exponential for large positive and negative z. In addition, as the only parameter in the game is varied, we find a transition where one player is able to get its maximum theoretical score. By extending this model, we suggest that the front velocity v is selected by the nonlinear marginal stability mechanism arising in some traveling wave problems for which the profile decays exponentially, and for which standard traveling wave theory applies.

DOI: 10.1103/PhysRevE.78.061106 PACS number(s): 02.50.−r, 05.40.−a

Extreme value statistics of random variables has been long studied by mathematicians [1,2] and physicists [3–5]. In physics, it naturally arises when studying thermodynamical properties of disordered systems [6], and, in particular, the distribution of the ground state energy [4,5].

If the considered random variables $E_1,E_2,\ldots,E_N$ are uncorrelated, the distribution of $E_{\min}=\min_i E_i$ or $E_{\max}=\max_i E_i$ becomes universal for large N, once properly scaled [1,2]. It takes the form of the Gumbel, Fréchet, or Weibull distribution depending on the asymptotic properties of the distribution of the E_i's. However, in the case of strongly correlated random variables, there are no general results, and it is usually a formidable task to access to the distribution of $E_{\min}$ or $E_{\max}$.

In [4], the authors study a simple model of a directed polymer on a Cayley tree, inspired from the original work of [6], but focusing on the ground state properties (i.e., zero temperature). The simplest version of the model is defined on a Cayley tree developed over n generations, and with Z branches originating from each node. The polymer made of n bonds starts from the root node, and for a given path on the tree, the total length of the polymer (assimilated to its energy) is

$$E_{\text{path}} = \sum_{i\in \text{path}} l_i. \tag{1}$$

The elementary lengths l_i are quenched random variables associated with each bond of the tree and independently drawn from the same random distribution $\rho(l)$. The hierarchical structure of the Cayley tree induces strong correlations between the different possible energies (or lengths) of the polymer. One is then interested in the distribution of the minimal energy $E_{\min}$, i.e., the ground state energy. Because of these strong correlations, the ground state energy distribution is not expected to fall into one of the three universality classes arising in the case of independent random variables [4,5], the best known of them being the Gumbel distribution [1,2]. In the special case of the binary distribution

$$\rho(l) = p\,\delta_{l,1} + (1-p)\,\delta_{l,0}, \quad p \in [0,1], \tag{2}$$

the authors of [4] obtained an unbinding transition when $p > p_c = 1 - Z^{-1}$, where the polymer goes from a finite length to an extensive length $\langle E_{\min}\rangle \sim v(p)n$. In addition, the distribution of $E_{\min}$ has a traveling front form

$$P(E_{\min},n) = f(E_{\min} - v(p)n), \tag{3}$$

where $f(z)$ decays exponentially fast for large negative argument. This last property and the general theory of traveling waves [7–11] lead to a simple selection mechanism for the front velocity $v(p)$ (linear marginal stability; see hereafter).

In the present work, we define a game theoretical model, directly inspired by this directed polymer model. Although our model lacks any thermodynamical reference, it is certainly related to other optimization problems, where the notions of extreme value statistics and traveling fronts arise [3].

Two players A and B play an alternating game of duration n, with player A starting the game. When it is its turn to play, a player has a choice of Z possible moves. Hence, the map of all possible game histories has the structure of a Cayley tree with Z branches originating from any node, and of length $2n$. The ith move by player A brings it the additional score a_i, whereas the next play by player B adds the value b_i to the score of player A. The score of player B is defined as the opposite of that of player A. The elementary scores a_i and b_i are quenched random variables independently drawn from the same distribution ρ. Ultimately, the final score of player A is

$$E_{\text{path}} = \sum_{i\in \text{path}} a_i + b_i. \tag{4}$$

The goal of player A is to maximize its final score, whereas player B will do its best to select its plays in order to minimize the score of player A, and hence maximize its own score. The two players have an *a priori* knowledge of the game tree structure so that the final score of player A is defined as

*clement.sire@irsamc.ups-tlse.fr

$$S_n = \max_{\text{available choices of } A} \min_{\text{available choices of } B} E_{\text{path}}. \quad (5)$$

From now, we specialize to the case $Z=2$, although our results can be easily extended to any Z. Moreover, we restrict ourselves to the elementary score distribution given by Eq. (2). It should be emphasized that the players do not pick their next play in order just to maximize its local outcome (i.e., A picking its next move among available branches with $a_i=1$ or B picks the minimum available b_i). If the players were adopting such a simple depth-0 strategy, which would be their natural approach if they did not have the prior knowledge of the a_i and b_i distribution over the tree, the final score of player A would be simply the sum of n independent variables of mean $p^2+2p(1-p)$ (A picks a branch with $a_i=1$, if there is one available), and n variables of mean p^2 (B picks a branch with $b_i=0$, if there is one available). Then the distribution of S_n would be a Gaussian (of width $\sigma \sim \sqrt{n}$), and mean $\langle S_n \rangle = v_0(p)n$, with

$$v_0(p) = p^2 + 2p(1-p) + p^2 = 2p. \quad (6)$$

Note that this result is identical to the score velocity obtained if the players had picked their move at random: the depth-0 strategies of both players exactly annihilate. Instead, having a global view of the game tree, the players will try to direct the game into favorable branches for them, in order to maximize their final score, even if they may have sometimes to pick an unfavorable local move ($a_i=0$ for player A, $b_i=1$ for player B) in order to achieve their goal. For $p>1/2$, there are more bonds with $a_i=1$ or $b_i=1$, so that we expect that the objective of player A should be easier to achieve than that of player B. Hence, we anticipate that $\langle S_n \rangle = v(p)n$, with

$$v(p) \geq v_0(p) = 2p, \quad p \geq \frac{1}{2}. \quad (7)$$

In the opposite case $p<1/2$, the above inequality is obviously reversed. In fact, by exchanging the roles of A and B (and neglecting the fact that A starts the game, for large n), it is clear that one has the symmetry relation [4]

$$v(p) + v(1-p) = 2. \quad (8)$$

In addition, one has the trivial constraints,

$$v(0) = 0, \quad v(1/2) = 1, \quad v(1) = 2, \quad (9)$$

which are consistent with Eq. (8).

An intermediate strategy to the ones presented above corresponds to players having only a partial view of the game tree up to a finite depth. For instance, if the players have the knowledge of there next available move, and of their opponent's ensuing options, they should adopt the following depth-1 strategy.

(1) Player A: if the options of player A are equal (both $a_i=0$ or 1), A picks the branch for which the number of b_i equal to 1 (when it is the turn of B to play) is maximal. If only one branch corresponds to $a_i=1$, A chooses this move.

(2) Player B: if the options of player B are equal (both $b_i=0$ or 1), B picks the branch for which the number of a_{i+1} equal to 1 is minimal. If only one branch corresponds to $b_i=0$, B picks this move.

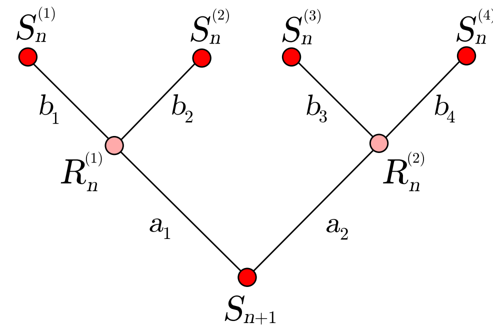

FIG. 1. (Color online) S_{n+1} can be obtained recursively from four optimized scores $S_n^{(k)}$ ($k=1,2,3,4$), and finding the next optimized move from player B and then from player A.

After an elementary but cumbersome calculation, we find that the score velocity $v_1(p)$ corresponding to this depth-1 strategy is given by

$$v_1(p) = 2p^2 \frac{7 - 6p + 4p^2 - 14p^3 + 14p^4 - 4p^5}{1 + 2p + 6p^2 - 16p^3 + 8p^4}. \quad (10)$$

One has $v_1(p) \geq v_0(p)$ for $p \geq 1/2$, and $v_1(p)$ satisfies the symmetry relation of Eq. (8) and the conditions of Eq. (9). For higher but finite strategy depth, an analytical treatment becomes extremely complicated.

Let us now move back to our model, where both players have a global knowledge of the game tree (infinite depth). Obtaining the (not necessarily unique) optimal path realizing both players antagonistic goals can be achieved by using the recursive MINIMAX algorithm [12], which gives a more precise meaning to Eq. (5). Let us assume that we have generated four instances of optimized scores $S_n^{(k)}$ ($k=1,2,3,4$) on four independent games of length n (with the initial condition $S_n^{(k)}=0$, for $n=0$). In order to construct an optimized score for a game of length $n+1$, we first generate two intermediate scores including the previous move of player B (see Fig. 1),

$$R_n^{(1)} = \min(S_n^{(1)} + b_1, S_n^{(2)} + b_2),$$

$$R_n^{(2)} = \min(S_n^{(3)} + b_3, S_n^{(4)} + b_4). \quad (11)$$

Then the final score is obtained by optimizing the first move of player A over his two possible plays a_1 and a_2 (see Fig. 1):

$$S_{n+1} = \max(R_n^{(1)} + a_1, R_n^{(2)} + a_2). \quad (12)$$

Using Eqs. (11) and (12), we can derive the corresponding recursion relations for the cumulative distribution of S_n and R_n,

$$P_n(m) = \text{Prob}(S_n \leq m),$$

$$Q_n(m) = \text{Prob}(R_n \leq m), \quad (13)$$

and starting from the initial condition $P_n(m)=1$ for $m \geq 0$, and $P_n(m)=0$ for $m<0$. Defining $q=1-p$, we find

$$Q_n(m) = 1 - [1 - qP_n(m) - pP_n(m-1)]^2, \quad (14)$$

$$P_{n+1}(m) = [qQ_n(m) + pQ_n(m-1)]^2. \tag{15}$$

The intermediate distribution $Q_n(m)$ can be eliminated by inserting Eq. (14) into Eq. (15), leading to a single recursion relation between P_{n+1} and P_n. The probability density of S_n is defined as

$$p_n(m) = P_n(m) - P_n(m-1). \tag{16}$$

We look for a traveling wave form for $P_n(m)$,

$$P_n(m) = F(m - \langle S_n\rangle), \quad \langle S_n\rangle = v(p)n, \tag{17}$$

with the boundary conditions $F(z)\to 1$, for $z\to +\infty$, and $F(z)\to 0$, for $z\to -\infty$. The probability density of S_n has a similar traveling wave form, associated with the hull function $f(z)$:

$$p_n(m) = f(m - \langle S_n\rangle), \quad f(z) = F(z) - F(z-1). \tag{18}$$

Inserting this ansatz into Eqs. (14) and (15), we find that F satisfies the following functional equation:

$$\sqrt{F(z-v)} = 1 - q[1 - qF(z) - pF(z-1)]^2 - p[1 - qF(z-1) - pF(z-2)]^2, \tag{19}$$

where we have used the shorthand notation v for $v(p)$. By retaining the leading contributions in Eq. (19) for $z\to -\infty$, and for $v>0$, we find

$$F(z-v) \sim 4q^4F^2(z), \tag{20}$$

which leads to the double exponential asymptotics

$$F(z) \sim f(z) \sim \frac{1}{4q^4}\exp(-\alpha_- 2^{|z|/v}), \tag{21}$$

where $\alpha_->0$ is an unknown p-dependent constant. Similarly, in the opposite limit $z\to +\infty$, and assuming $v<2$, the functional equation (19) reduces to

$$1 - F(z-v) \sim 2p^3[1 - F(z-2)]^2, \tag{22}$$

which again leads to a double exponential decay

$$1 - F(z-1) \sim f(z) \sim \frac{1}{2p^3}\exp(-\alpha_+ 2^{z/(2-v)}), \tag{23}$$

where $\alpha_+>0$ is some p-dependent constant. Hence, and contrary to the standard traveling wave theory [3–5], where the traveling front exponential decay for $z\to -\infty$ or $z\to +\infty$ permits the determination of the front velocity, $v(p)$ remains so far undetermined. Here, the double exponential decay obtained on both sides results from the MINIMAX constraint, instead of the usual MIN (or MAX) constraint imposed when considering the ground state energy or the minimum (or maximum) path length distribution [4,5]. This fast decay of $f(z)$ for $z\to \pm\infty$ and the traveling wave form of Eq. (18) ensure that $\langle [S_n - v(p)n]^2\rangle$ remains bounded when $n\to +\infty$.

$v(p)$ can still be determined numerically, from its definition $\langle S_n\rangle = v(p)n$. The results are shown in Fig. 2, along with $v_0(p)$ and $v_1(p)$ which correspond to depth-0 and depth-1 strategies respectively. The main feature of $v(p)$ is the existence of a critical value of p (denoted p_c), above which the score front velocity is $v(p)=2$ [note that one also has $v_1'(1)=0$]. Moreover, and as mentioned above, $v_0(p)$ is a lower bound of $v(p)$. Finally, for p close to $1/2$, $v(p)$ grows linearly with p, with

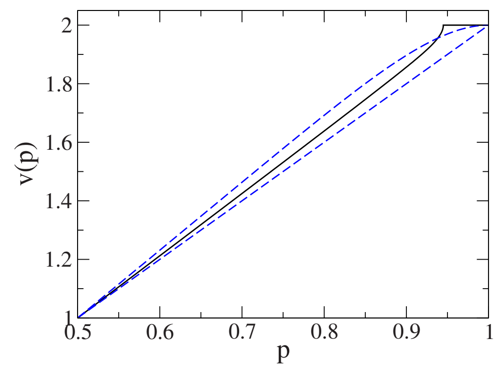

FIG. 2. (Color online) We plot the score velocity front $v(p)$ (full line), the lower bound $v_0(p)=2p$ (lower dashed line), and $v_1(p)$, obtained when the players adopt a depth-1 strategy (upper dashed line). For $p<1/2$, $v(p)$ is obtained by symmetry, using Eq. (8). The heuristic expression of Eq. (30) cannot be distinguished from the numerical data at this scale.

$$v_0'(1/2) = 2,$$

$$v'(1/2) \approx 2.123(1),$$

$$v_1'(1/2) = \frac{37}{16} = 2.3125. \tag{24}$$

In the symmetric case $p=1/2$, we find that $\langle S_n\rangle = n+\sigma_0$, where $\sigma_0=0.142\,916\,95\ldots$ is a strictly positive constant, illustrating the slight advantage that A gains from starting the game.

Let us give a physical explanation for the occurrence of this transition. As $p>1/2$ increases, the number of paths along which all the a_i's and b_i's are equal to 1 grows exponentially. Indeed, the probability of having such a path is p^{2n}, so that their total number in the tree is of order $2^{2n}\times p^{2n}$. The existence of this transition shows that, for $p>p_c$, player A is able to chose his moves in order to force the outcome of the game to follow one of these path, with probability unity, as $n\to\infty$. Symmetrically, for $p<1-p_c$, player B will find enough branches along which most a_i's and b_i's are equal to 0, in order to enforce that the front velocity remains zero in this regime, consistently with the symmetry relation of Eq. (8).

This transition can be understood analytically, by studying the stability of a traveling front of velocity $v(p)=2$. Noting that $P_n(2n)=Q_n(2n+1)=1$ (since $S_n\leqslant 2n$ and $R_n\leqslant 2n+1$), we consider the dynamics of $u_n=P_n(2n-1)\leqslant 1$. From Eqs. (14) and (15), u_n satisfies the recursion relation

$$u_{n+1} = [1 - p^3(1-u_n)^2]^2, \tag{25}$$

with $u_0=0$. $u_n=P_n(2n-1)=1$ is an obvious fixed point of Eq. (25), corresponding to the case $v(p)<2$. If this fixed point is selected, and after linearizing Eq. (25), we find that

$$\ln[1 - P_n(2n-1)] \sim -2^n, \quad (26)$$

which is fully consistent with Eq. (23), with $z=2n-1-v(p)n$. However, the recursion relation of Eq. (25) has three other fixed points (x_-,x_+,x_0), which can be obtained analytically by solving a third-order polynomial equation, leading to cumbersome expressions. A detailed analysis shows that x_0 is always real, with $x_0>1$. This fixed point is unphysical and necessarily unstable. The two other fixed points are real for $p \geqslant p_c$ $(x_- < x_+)$, with

$$p_c = \frac{3}{4} \times 2^{1/3} = 0.944\,94\ldots, \quad (27)$$

and complex conjugates for $p<p_c$. Moreover, one finds that x_- is maximal for $p=p_c$, at which $x_\pm = 1/9$. Finally, a stability analysis shows that x_- is the only stable fixed point for $p_c < p \leqslant 1$. Hence, we conclude that $P_n(2n-1)$ converges (exponentially fast) to x_- for $p_c<p\leqslant 1$, and that the distribution of S_n is peaked near $m=2n$ and decays as a double exponential for $m \ll 2n$ [as given by Eq. (21)], leading to $v(p)=2$. The obtained value of p_c is in perfect agreement with the numerical results for $v(p)$ plotted on Fig. 2. Close to $p=1$, $x_- \sim 9(1-p)^2 \to 0$, and up to second order in $(1-p)$, the distribution of S_n is thus given by

$$p_n(2n) = 1 - 9(1-p)^2, \quad p_n(2n-1) = 9(1-p)^2. \quad (28)$$

Note that, if both players adopt a finite depth strategy, this transition does not occur, as illustrated in Fig. 2 in the case of the depth-0 and depth-1 strategies considered above. By adopting a short-sighted strategy, player A (B) cannot direct, with probability 1, the sequence of plays to a branch of the tree with a density unity of playing options $a_i=b_i=1$ $(a_i=b_i=0)$.

Finally, for p below but close to p_c, we obtain a very convincing fit of $v(p)$ to the functional form

$$v(p) = 2 - c(p_c - p)^{1/2} + \cdots, \quad (29)$$

with $c \approx 0.50(1)$, leading to an infinite slope for $v(p)$ at $p=p_c^-$, as found numerically on Fig. 2. In fact, for $p \geqslant 1/2$, we find that the simple heuristic functional form

$$v(p) = 2 - 2\left(\frac{(p_c-p)(1-p)}{2p_c-1}\right)^{1/2} \quad (30)$$

fits the data with a relative accuracy better than 0.1%, comparable with although slightly higher than the estimated numerical error bars of the data. This functional form ensures that $v(1/2)=1$ and that the behavior of Eq. (29) is reproduced, and leads to the heuristic values

$$v'(0) = 2.120\,99\ldots, \quad c = 0.497\,48\ldots, \quad (31)$$

in good agreement with the numerical estimates presented above.

Let us now address the properties of the hull function $f(z)$, and its cumulative sum $F(z)$. First of all, if for a given p, the corresponding $v(p)$ happens to be a rational number $v(p)=\alpha/\beta$ (α and β being mutually prime), Eq. (19) implies that the hull function is only defined on the discrete set of fractions of the form k/β. This is in particular the case for $p=1/2$ $[v(1/2)=1]$, $p>p_c$ $[v(p)=2]$, and $p<1-p_c$ $[v(p)=0]$. On the other hand, when $v(p)$ is irrational, the set of points of the form $z=m-v(p)n$ is dense on the real axis, and $f(z)$ is a continuous function defined on the real axis. As $v(p)$ approaches $v(p_c)=2$ from below, the hull function $f(z)$ develops steps which blend into discontinuities as $p\to p_c$. This property is illustrated in Fig. 3, along with the asymptotics obtained in Eqs. (21) and (23).

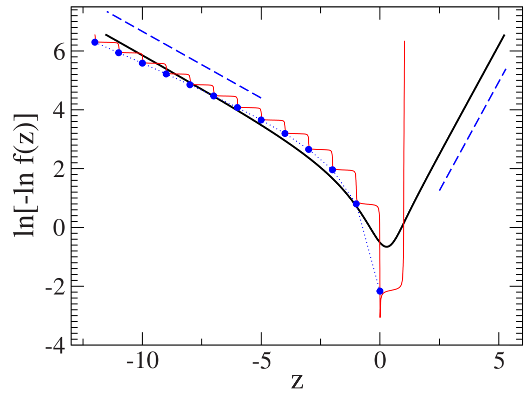

FIG. 3. (Color online) Hull function $f(z)$ for $p=0.944\,95>p_c$, for which $v(p)=2$, and which is defined on negative integer values of z (dots linked by a dotted line). For $p=0.9449$ slightly below p_c $[v(p)=1.996\,84\ldots]$, the hull function is continuous but exhibits smooth steps at integer values of z (corresponding thin line). Finally, for $p=0.75$ $(v(p)=1.531\,46\ldots)$, we plot the continuous hull function (thick line) along with the predicted asymptotics of Eqs. (21) and (23) (dashed lines).

We now extend our original model in order to gain some insight into the velocity selection mechanism. This is achieved by modifying the model so that the standard theory of front propagation will apply. In this (A,ε) model, player A always follows its best strategy, while player B follows the depth-0 strategy (picking a branch with $b_i=0$ if available) with probability ε and its optimal strategy with probability $1-\varepsilon$. The original model is hence recovered for $\varepsilon=0$. The recursion relation of Eq. (14) now becomes

$$Q_n(m) = (1-\varepsilon)\{1 - [1 - qP_n(m) - pP_n(m-1)]^2\} + \varepsilon[(q^2+2pq)P_n(m) + p^2P_n(m-1)], \quad (32)$$

while Eq. (15) remains unchanged. We denote the associated front velocity by $v_A(p,\varepsilon)$. Note that, if B is playing purely randomly, the terms q^2+2pq and p^2 in Eq. (32) must be replaced, respectively, by q and p. This model has exactly the same qualitative properties as the (A,ε) model, on which we hence concentrate, since player B adopts a more intelligent strategy (some results obtained for the random model will be mentioned in passing). In the (B,ε) model, one exchanges the role of players A and B, and Eq. (15) is changed into

$$P_{n+1}(m) = (1-\varepsilon)[qQ_n(m) + pQ_n(m-1)]^2 + \varepsilon[q^2Q_n(m) + (p^2+2pq)Q_n(m-1)], \quad (33)$$

whereas Eq. (14) still holds. When exchanging the role of the two players, the associated front velocity $v_B(p,\varepsilon)$ satisfies the symmetry relation

$$v_A(p,\varepsilon)+v_B(1-p,\varepsilon)=2, \tag{34}$$

which reduces to Eq. (8), when $\varepsilon=0$. However, for $\varepsilon>0$, $v_A(p,\varepsilon)$ and $v_B(1-p,\varepsilon)$ do not obey the symmetry relation of Eq. (8). In addition, we have the exact inequalities

$$v_B(p,\varepsilon)\leqslant v(p)\leqslant v_A(p,\varepsilon), \tag{35}$$

since players B and A are, respectively, playing less optimally in the (A,ε) and (B,ε) models than in the original model.

Because of the symmetry relation of Eq. (34), we focus on the (A,ε) model, and denote the associated velocity simply by v. The (A,ε) model's main interest lies in the fact that for $\varepsilon>0$ $\bar{P}_n(m)=1-P_n(m)$ decays exponentially for $m\gg vn$, so that the standard mechanisms of front velocity selection do apply (see below). When $\bar{P}_n(m)\ll 1$, the recursions of Eqs. (15) and (32) indeed lead to

$$\bar{P}_{n+1}(m)=2\varepsilon[(1+p)(1-p)^2\bar{P}_n(m)+p(1-p)(2p+1)\bar{P}_n(m-1)+p^3\bar{P}_n(m-2)], \tag{36}$$

or, equivalently, the front profile $\bar{F}(z)=1-F(z)$ satisfies

$$\bar{F}(z-v)=2\varepsilon[(1+p)(1-p)^2\bar{F}(z)+p(1-p)(2p+1)\bar{F}(z-1)+p^3\bar{F}(z-v)], \tag{37}$$

to be compared to Eq. (22), for the original model. The simple ansatz $\bar{F}(z)\sim\exp(-\lambda z)$ leads to the dispersion relation

$$v(\lambda)=\frac{1}{\lambda}\ln[2\varepsilon(1-p+pe^{\lambda})(1-p^2+p^2e^{\lambda})], \tag{38}$$

where the decay rate λ is so far undetermined.

Let us now summarize the main known mechanisms of velocity front selection [7–11] for exponentially fast decaying profiles. In many physical cases, including those studied in [4,5], a linear marginal stability (LMS) argument shows that the selected front velocity corresponds to the minimum velocity $v_{\min}$ allowed by the dispersion relation $v(\lambda)$, associated with the decay rate $\lambda_{\min}$. However, in some other cases [9–11], a bigger velocity is selected by a nonlinear marginal stability (NLMS) mechanism. Without entering into too much detail, let us briefly explain this point. Consider the large-z asymptotics of a solution of the full nonlinear problem associated to the velocity v,

$$\bar{F}(z)\sim A_1(v)e^{-\lambda_1(v)z}+A_2(v)e^{-\lambda_2(v)z}+\cdots, \tag{39}$$

with $\lambda_1(v)<\lambda_{\min}$ given by the dispersion relation derived from linear analysis. Note that the above linear analysis does not grant access to $A_1(v)$, not to mention the correction term proportional to $A_2(v)$. Now, if there exists a velocity $v_*>v_{\min}$ for which $A_1(v_*)=0$, $\bar{F}(z)$ will decay more sharply with rate $\lambda_2(v_*)$, which is necessarily another root of the dispersion relation, with $\lambda_2(v_*)>\lambda_{\min}$. It can be shown that all traveling fronts with velocity less than v_* are then unstable against invasion by a profile of velocity v_*, which leads to the selection of the velocity front v_*, instead of $v_{\min}$ [9–11]. In practice, there are very few examples for which the transition between a linear and a nonlinear marginal stability scenario can be analytically identified, since it requires in general a full solution of the profile associated to a velocity v, in order to obtain $A_1(v)$. To the knowledge of the author, all such tractable examples concern traveling fronts in the spatial and temporal continuum [9–11], like, for instance,

$$\frac{\partial P}{\partial t}=\frac{\partial^2 P}{\partial x^2}+P(1-P)(1+\kappa P), \tag{40}$$

for $\kappa\geqslant 1$. In this case [9,11], $v(\lambda)=\lambda+\lambda^{-1}$, so that $v_{\min}=2$ and $\lambda_{\min}=1$. $v_{\min}$ is selected for $1\leqslant\kappa\leqslant 2$, whereas $v=v_*=(\kappa/2)^{1/2}+(\kappa/2)^{-1/2}$ [with $\lambda_1=(\kappa/2)^{-1/2}$ and $\lambda_2=(\kappa/2)^{1/2}$], for $\kappa>2$.

Returning to our (A,ε) model, we find that a nontrivial $v_{\min}$ exists for any $\varepsilon>1/2$. It is obtained by first finding $\lambda_{\min}$, the unique real positive solution of

$$v'(\lambda_{\min})=0, \tag{41}$$

and setting $v_{\min}=v(\lambda_{\min})$ in Eq. (38). In particular, we find that $v_{\min}=2$, for $p>p_c$, with

$$p_c=(2\varepsilon)^{-1/3}. \tag{42}$$

In the case $\varepsilon=1$, when player B always adopts the depth-0 strategy, we find $p_c=2^{-1/3}=0.793\,700\,5\ldots$. Hence, we obtain the same kind of transition as in the original model, where player A is able to get its maximum theoretical score. However, since B has a short-sighted strategy, we do not observe a transition to $v=0$ for small but nonzero p, as obtained in the original model for $p=1-p_c$. We actually find $v_{\min}\sim -\ln(2\varepsilon)/\ln(p)$, when $p\to 0$. Note that if B plays randomly instead of adopting the depth-0 strategy, we obtain the dispersion relation

$$v(\lambda)=\frac{1}{\lambda}\ln[2\varepsilon(1-p+pe^{\lambda})^2], \tag{43}$$

and $p_c=(2\varepsilon)^{-1/2}$.

However, for a given p, we find numerically that the velocity given by the LMS mechanism $v_{\min}$ is selected only for $\varepsilon\geqslant\varepsilon_c(p)$, so that the results of Eqs. (38), (41), and (42) are valid only for ε close enough to 1. For $1/2<\varepsilon<\varepsilon_c(p)<1$, and although a nontrivial $v_{\min}$ does exist, we find $v>v_{\min}$. This strongly suggests the relevance of the NLMS mechanism in this case. Unfortunately, for $1/2<\varepsilon<\varepsilon_c(p)$ and a given v, there is very little hope of obtaining an analytical solution of the corresponding full nonlinear equation for $F(z)$, in order to apply the NLMS criterion explained above. Likewise, for $\varepsilon<1/2$, the minimal positive velocity is $v_{\min}=0$ $(v(\lambda=0)=-\infty)$, and the prospect of an analytical solution appears even bleaker. Note however that v and the associated decay rate λ are still related by the dispersion relation of Eq. (38).

On the bright side, the full line $p_c(\varepsilon)$ can be determined exactly, by studying the dynamics of $u_n=1-P_n(2n-1)$, in the same spirit as in the case $\varepsilon=0$. We find that u_n satisfies the exact recursion relation

$$u_{n+1} \equiv g_{p,\varepsilon}(u_n) = z_n(2-z_n), \quad (44)$$

$$z_n = p^3 u_n[\varepsilon + (1-\varepsilon)u_n], \quad (45)$$

with $u_0=1$. We then determine the value of $p_c(\varepsilon)$ above which there exists a stable nontrivial fixed point $u_*(\varepsilon)\neq 0$. For $\varepsilon \geqslant 4/5$, we find that $p_c(\varepsilon)$ is indeed given by the LMS argument, leading to the result of Eq. (42). On the other hand, for $0 \leqslant \varepsilon < 4/5$, a regime where the NLMS mechanism should be relevant, $p_c(\varepsilon)$ and $u_*(\varepsilon)$ are determined in the same spirit as in the case $\varepsilon=0$, by imposing the condition that $g_{p_c,\varepsilon}(u_*)/u_* - 1 = g'_{p_c,\varepsilon}(u_*) - 1 = 0$. We find

$$p_c(\varepsilon) = \left(\frac{(1-\varepsilon)^{1/2}(4-\varepsilon)^{3/2} - 8 + 7\varepsilon + \varepsilon^2}{2\varepsilon^2} \right)^{1/3}, \quad (46)$$

which goes smoothly to the result of Eq. (27), when $\varepsilon \to 0$.

Interestingly, this analysis provides the exact value of ε_c for the corresponding value of $p=p_c(\varepsilon_c)=(2\varepsilon_c)^{-1/3}$, at the transition between the LMS and NLMS regimes. We thus find

$$\varepsilon_c\left(p = \frac{5^{1/3}}{2} = 0.854\,988\ldots\right) = \frac{4}{5}. \quad (47)$$

If B plays randomly instead of adopting the depth-0 strategy, one obtains

$$\varepsilon_c\left(p = \frac{1+\sqrt{5}}{4} = 0.809\,017\ldots\right) = 3 - \sqrt{5} = 0.763\,932\ldots. \quad (48)$$

In Fig. 4, we plot our exact result for $p_c(\varepsilon)$ and a numerical estimate of $\varepsilon_c(p)$, the boundary between the LMS and NLMS domains of application. In Fig. 5, we plot $v_A(p,\varepsilon)$ and $v_B(p,\varepsilon)$ for $\varepsilon=1$, where B and A are respectively adopting the depth-0 strategy, for $\varepsilon=4/5$, the smallest ε for which the LMS mechanism applies for all p, and for $\varepsilon=1/4$, for which the NLMS mechanism holds for all p. We observe numerically that $v_A(p,\varepsilon)$ and $v_B(p,\varepsilon)$ converge smoothly to $v(p)$ as $\varepsilon \to 0$.

Let us finally address the subleading corrections to the average score $\langle S_n\rangle$. The LMS mechanism implies [7,10] that

$$\langle S_n\rangle = v_{\min} n - \frac{3}{2\lambda_{\min}} \ln n + \cdots. \quad (49)$$

In the (ε,p) regime where the LMS mechanism applies, we have confirmed numerically the occurrence of this logarithmic correction, as well as its magnitude. In the NLMS regime, we find instead that the next correction to $\langle S_n\rangle = vn$ is constant. Quite generally, this result can be justified analytically whenever $v > v_{\min}$, in particular when the NLMS mechanism applies [13]. This property was exploited in order to obtain the numerical estimate of $\varepsilon_c(p)$ shown in Fig. 4, and this criterion is found to be fully consistent with defining $\varepsilon_c(p)$ as the value of ε for which v becomes equal to the velocity $v_{\min}$ selected by the LMS mechanism [see Eqs. (38), (41), and (42)].

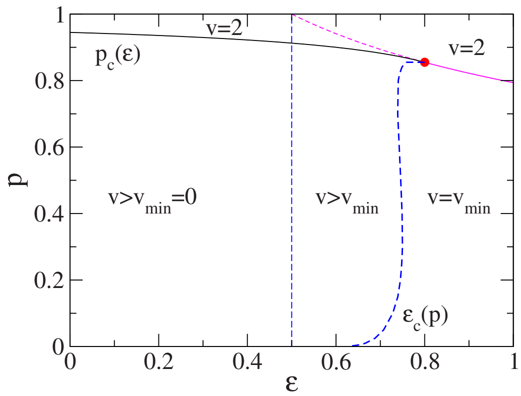

FIG. 4. (Color online) We plot the exact $p_c(\varepsilon)$ above which $v_A(p,\varepsilon)=2$ (full line), whose LMS and NLMS expressions are respectively given by Eqs. (42) and (46). We also plot the numerical estimate of $\varepsilon_c(p)$ (thick dashed line), the boundary between the LMS and NLMS domains of application. These two curves cross at $(\varepsilon_c,p_c)=(4/5,5^{1/3}/2)$ (dot). We also identify three domains according to the relation between the observed front velocity v and the LMS velocity $v_{\min}$.

In the present work, we have defined a simple two-player game inspired by a model of a directed polymer on the Cayley tree. The fact that the two players have antagonist goals is reminiscent of the notion of *frustration* quite common in disordered physical systems. In our model, this frustration originates from the MINIMAX constraint, which is, however, quite uncommon in physics. As a consequence, the present model has no thermodynamical interpretation. We found that the score distribution develops a traveling wave form, with the hull function unusually decaying superexponentially for large negative and positive arguments. We have justified analytically the occurrence of a transition, across which a player can obtain its maximum theoretical score, whatever the strategy of the other player. In contrast to systems for which the standard traveling wave theory applies, we did not succeed in understanding analytically the process which leads to the

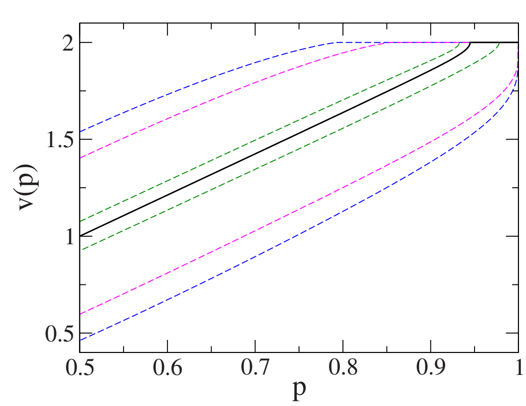

FIG. 5. (Color online) We plot the velocities $v_A(p,\varepsilon)$ (three upper dashed lines, $\varepsilon=1,4/5,1/4$ from top) and $v_B(p,\varepsilon)$ (three lower dashed lines, $\varepsilon=1,4/5,1/4$ from bottom). The full line corresponds to $v(p)$ for the original model ($\varepsilon=0$).

selection of the velocity front. However, after studying an extension of the original model, we strongly suggest that the selection mechanism is related to nonlinear marginal stability, arising in some traveling wave problems for which the profile decays exponentially.

ACKNOWLEDGMENTS

I am very grateful to Satya Majumdar for fruitful discussions. I also wish to thank a referee for suggesting studying a model where only one player is adopting the optimal strategy, whereas the other plays randomly.

[1] E. J. Gumbel, *Statistics of Extremes* (Columbia University Press, New York, 1958).
[2] J. Galambos, *The Asymptotic Theory of Extreme Order Statistics* (Krieger, Malabar, FL, 1987).
[3] P. L. Krapivsky and S. N. Majumdar, Phys. Rev. Lett. **85**, 5492 (2000).
[4] S. N. Majumdar and P. L. Krapivsky, Phys. Rev. E **62**, 7735 (2000).
[5] D. S. Dean and S. N. Majumdar, Phys. Rev. E **64**, 046121 (2001).
[6] B. Derrida and H. Spohn, J. Stat. Phys. **51**, 817 (1988); B. Derrida, Phys. Scr., T **38**, 6 (1991).
[7] M. Bramson, *Convergence of Solutions of the Kolmogorov Equation to Traveling Waves* (American Mathematical Society, Providence, RI, 1983).
[8] G. Dee and J. S. Langer, Phys. Rev. Lett. **50**, 383 (1983).
[9] E. Ben-Jacob, H. R. Brand, G. Dee, L. Kramer, and J. S. Langer, Physica D **14**, 348 (1985).
[10] D. G. Aronson and H. F. Weinberger, in *Partial Differential Equations and Related Topics*, edited by J. A. Goldstein (Springer, Heidelberg, 1975); Adv. Math. **30**, 33 (1978).
[11] W. van Saarloos, Phys. Rev. A **39**, 6367 (1989).
[12] S. J. Russell and P. Norvig, *Artificial Intelligence: A Modern Approach*, 2nd ed., Series in Artificial Intelligence (Prentice-Hall, Upper Saddle River, NJ, 2002).
[13] C. Sire (unpublished).